Available online at www.sciencedirect.com
ScienceDirect
International Journal of Heat and Mass Transfer 50 (2007) 2667–2674
International Journal of HEAT and MASS TRANSFER
www.elsevier.com/locate/ijhmt

On the heat transfer characteristics of heat sinks: Influence of fin spacing at low Reynolds number region

Kai-Shing Yang [a,*], Ching-Ming Chiang [b], Yur-Tsai Lin [b], Kuo-Hsiang Chien [a], Chi-Chuan Wang [a]

[a] *Energy and Environment Laboratories, Industrial Technology Research Institute, Hsinchu 310, Taiwan*
[b] *Mechanical Engineering Department, Yuan-Ze University, Taoyuan 320, Taiwan*

Received 8 June 2006; received in revised form 22 November 2006

Abstract

This study examines the thermal–hydraulic performance of heat sinks having plate, slit, and louver fin patterns. Comparison of the associated heat transfer performance and the effect of fin spacing are made. The results indicate that the enhanced fin patterns like louver or slit fin operated at a higher frontal velocity and at a larger fin spacing is more beneficial than that of plain fin geometry. The heat transfer performance of louver fin is usually better than that of slit fin but accompanies with higher pressure drops. However, it is found that the pressure drops for slit fin is comparable to the louver fin geometry when the fin spacing is reduced to 0.8 mm. This is associated with the appreciable rise of entrance/exit loss (form drag) caused by the slit fin geometry. The test results also reveal a significant drop of heat transfer performance at a low Reynolds number and at a small fin spacing, or the so-called "maximum" phenomenon of Colburn j factor. This is applicable to all the tested geometries. By a careful examination of the test results, it is concluded that this phenomenon is related to the developing/fully developed flow characteristics. In fact, the maximum point occurred roughly at $x^+ = 0.1$ where fully developed and developing flow is separated.
© 2007 Elsevier Ltd. All rights reserved.

Keywords: Louver; Slit; Plate; Heat sink; Inverse Graetz number

1. Introduction

With the advance of electronic products showing significant performance improvements and versatile capability, the associated heat generation is also being dramatically increased. Hence the risk of failure and performance loss is increasing for the electronic devices, and sometimes may lead to a system failure. Therefore, thermal management is one of the major reliability concerns. There are many methods applicable to electronic cooling such as liquid cooling, air cooling, refrigeration, thermoelectric, and the like. Among them, air cooling is still the most popular one for its simplicity and low cost. One of the common arrangements of air cooling is via forced convection of the heat sink to dissipate heat from heat sources. Two most common fin patterns of the heat sink are plate and pin fin. The major advantages of these fin patterns are easy machining, simple structure and low cost.

Heat transfer and flow phenomena in plate and pin fin have been studied extensively. Sparrow et al. [1] experimentally examined the forced convection of plate fin array. Bar-Cohen and Rohsenow [2] developed a composite relation for the variation of heat transfer coefficient along the parallel plate surface for optimization of fins spacing, and the studies [3–6] were carried out to study the design and optimization of plate fin heat sinks. Narasimhan and Bar-Cohenm [7] showed the results based on an extensive set of CFD simulations for a three parallel plate heat sinks channel covering two distinct heat sink geometries, air velocities ranging from 0.25 m s^{-1} to 2 m s^{-1} at various spacings. Boesmans et al. [8] performed an experimental

* Corresponding author.
E-mail address: ksyang@itri.org.tw (K.-S. Yang).

0017-9310/$ - see front matter © 2007 Elsevier Ltd. All rights reserved.
doi:10.1016/j.ijheatmasstransfer.2006.11.047

Nomenclature

A_o	heat transfer surface area (m^2)
A_c	cross sectional area at the test section (m^2)
A_{fr}	frontal area of fins (m^2)
Cp_a	specific heat at constant pressure of air ($J\ kg^{-1}\ K^{-1}$)
D_h	hydraulic diameter (m^2)
f	friction factor (dimensionless)
F_p	fin pitch (m) = F_s + fin thickness
F_s	fin spacing (m)
$\bar{h}$	average convective heat transfer coefficient ($W\ m^{-2}\ K^{-1}$)
h_0	effective heat transfer coefficient ($W\ m^{-2}\ K^{-1}$)
j	Colburn factor (dimensionless)
k	thermal conductivity of air ($W\ m^{-1}\ K^{-1}$)
K_c	contraction loss coefficient (dimensionless)
K_e	expansion loss coefficient (dimensionless)
L	duct length (m)
L_h	louver height (m)
L_l	louver length (m)
L_p	louver pitch (m)
N	number of fins (dimensionless)
Nu	Nusselt number (dimensionless)
Pr	Prandtl number (dimensionless)
$\dot{Q}_{conv}$	convention heat transfer rate (W)
Re_{dh}	duct Reynolds number (dimensionless)
S_h	slit height (m)
S_w	slit width (m)
T_{avg}	the average temperature of the air (K)
T_w	the average surface temperature (K)
V	average air velocity ($m\ s^{-1}$)
V_c	the mean velocity in the flow channel ($m\ s^{-1}$)
V_{fr}	the frontal velocity ($m\ s^{-1}$)
x^+	inverse Graetz number (dimensionless)

Greek symbols

ΔP	total pressure drop (Pa)
ΔP_e	expansion pressure drop (Pa)
ΔP_f	friction pressure drop (Pa)
ΔP_i	entrance pressure drop (Pa)
α	aspect ratio of rectangular section (dimensionless)
σ	ratio of free-flow area to frontal area (dimensionless)
μ	dynamic viscosity ($kg\ m\ s^{-1}$)
ρ	density of air ($kg\ m^{-3}$)
θ	louver angle (deg)

comparison between plate fin heat sinks and staggered strip fin sinks.

Despite the popularity of plate fin heat sink, the performance of the plate fin surface may be inferior to interrupted surfaces. This is because that interrupted surfaces can provide better flow mixing and restart boundary layer. In that regard, if size limitation or effective heat removal are the main design concerns of electronic devices, it usually resorts to interrupted surfaces. Typical examples of interrupted surfaces are the slit fin and louver fin. The design of slit and louver fin is widely using in heat exchanger [9,10] which generally involves heat exchange between air and cooling working fluid within tube. This simulate a heat transfer condition of the fin surface at a near constant temperature situation. However, for electronic cooling applications where heat sink is commonly adhered to a constant heat source which simulates the condition of constant heat flux, some difference may exists between these two configuration. In addition, for applications involving augmented surfaces like louver, slit fin geometries or even the plain plate fin, very dense fin spacing is often encountered for providing more heat transfer surfaces. Hence, heat dissipation is often designed at low velocity region to prevent the penalty of high pressure drop. It is found in the subsequent results that a considerable performance drop prevails at this low Reynolds number region. Therefore, it is the main objective of this study to examine the influence of fin spacing on the air side performance of heat sinks at low Reynolds number region.

2. Experimental apparatus

The experiment apparatus is based on ASHRAE wind tunnel setup to measure the heat transfer and the pressure drop characteristics of the heat sink. Two main parts of the experimental apparatus is described below.

As seen in Fig. 1, experiments were performed in an open type wind tunnel. The ambient air flow was forced across the test section by a centrifugal fan with an inverter. To avoid and minimize the effect of flow maldistribution in the experiments, an air straightener-equalizer and a mixer were provided. The inlet and the exit temperatures across the sample were measured by two T-type thermocouple meshes. The inlet measuring mesh consists of four thermocouples while the outlet mesh contains eight thermocouples. The sensor locations inside the rectangular duct were established following ASHRAE [11] recommendation. These data signals were individually recorded and then averaged. During the isothermal test, the variation of these thermocouples was within 0.2 °C. In addition, all the thermocouples were pre-calibrated by a quartz thermometer having 0.01 °C precision. The accuracies of the calibrated thermocouples are of 0.1 °C. The pressure drop of the test sample and nozzle was detected by a precision differential pressure transducer, reading to 0.1 Pa. The air flow measuring station was a multiple nozzle code tester based on the ASHRAE 41.2 standard [12]. All the data signals are collected and converted by a data acquisition system (a hybrid recorder). The data acquisition system then

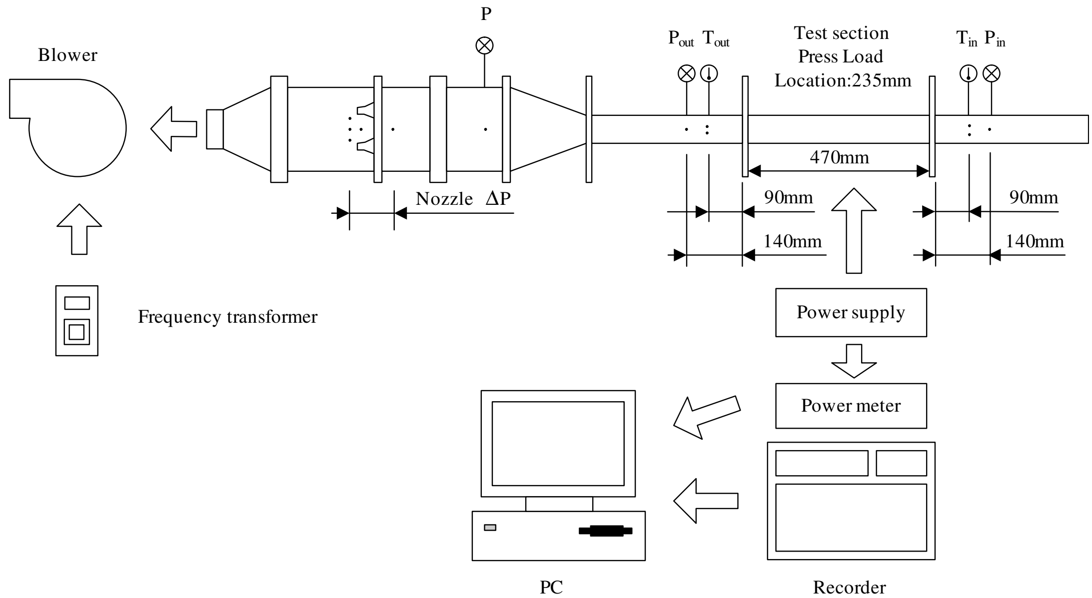

Fig. 1. Experimental setup.

transmitted the converted signals through Ethernet interface to the host computer for further operation.

A total of nine heat sinks were made and tested, the corresponding fin patterns are (a) plate fin; (b) louver fin; and (c) slit fin. The heat sinks are made from copper with thermal conductivity of 398 W m^{-1} K^{-1}. The geometries of heat sink are shown in Fig. 2, and their detailed dimensions are tabulated in Table 1. The base plates of the heat sinks

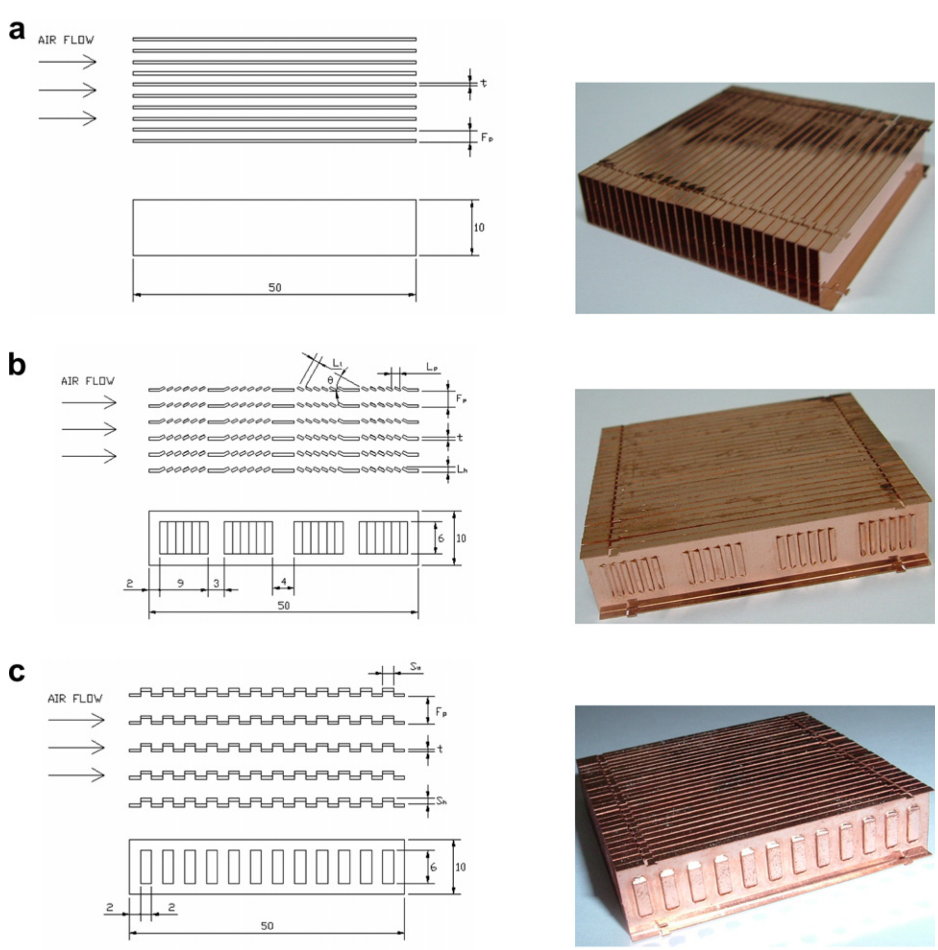

Fig. 2. Schematic of heat sinks geometry, (a) plate fin, (b) louver fin, and (c) slit fin.

Table 1
Detailed geometry of the heat sink (Unit: mm)

Fin type	Pitch (F_P)	Number of fins (N)	Louver height (L_h)	Louver length (L_l)	Louver pitch (L_P)	Louver angle (θ)	Slit height (S_h)	Slit width (S_w)
Plate	1.00	50	–	–	–	–	–	–
Plate	1.85	27	–	–	–	–	–	–
Plate	2.63	19	–	–	–	–	–	–
Louver	1.00	50	0.7	1	1.5	30°	–	–
Louver	1.85	27	0.7	1	1.5	30°	–	–
Louver	2.63	19	0.7	1	1.5	30°	–	–
Slit	1.00	50	–	–	–	–	0.5	2
Slit	1.85	27	–	–	–	–	0.5	2
Slit	2.63	19	–	–	–	–	0.5	2

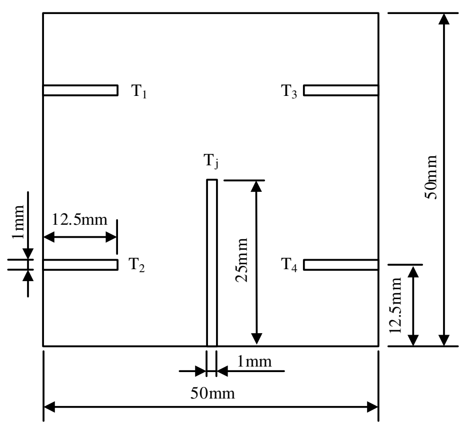

Fig. 3. Detailed locations of the thermocouples placed beneath the base plate.

are of square configuration with a length/width of 50 mm and a thickness of 2 mm. The corresponding fin pitches are 1.0, 1.85, 2.63 mm respectively with a constant fin thickness of 0.2 mm. In addition, the height of the heat sinks is 10 mm. A film heater with the same size of base plate is attached to the bottom of heat sink. During the tests, electric power supply provided 25 W power input to the heater. For measurement of the base temperature of heat sink, five temperature sensor signals were individually recorded and then averaged. Detailed locations of the thermocouples are shown in Fig. 3. The bakelite board is installed beneath the film heater in order to minimizing the heat loss. The heat sinks were loaded to a constant force of 11 N for all experiment. This provided consistent thermal contact resistance between the heat sinks and heater.

3. Analysis of heat sink

3.1. Pressure drop

For determination of the friction factor of the test samples, an adiabatic test is performed to obtain the total pressure drops. Therefore the pressure drops across the flow channel can be divided into three parts. Namely, the pressure drop at the entrance, pressure drop within the heat sink, and the expansion loss of the pressure drop at the exit of the rectangle channel

$$\Delta P = \Delta P_i + \Delta P_f + \Delta P_e \tag{1}$$

The entrance pressure drop of ΔP_i is often in terms of the pressure loss coefficient K_c, i.e.

$$\Delta P_i = \frac{1}{2}\rho V_c^2(1 - \sigma^2 + K_c) \tag{2}$$

where V_c is the mean velocity within the flow channel, $\sigma = A_c/A_{fr}$ denotes the contraction ratio. The expansion loss ΔP_e at the exit in terms of the pressure loss coefficient K_e

$$\Delta P_e = -\frac{1}{2}\rho V_c^2(1 - \sigma^2 - K_e) \tag{3}$$

Detailed values of the entrance and exit loss coefficient K_c and K_e can be estimated from the monograph of Kays and London [13]. Hence, the measured friction factor can be obtained from the following equation [13]:

$$f = \frac{\Delta P - \Delta P_i - \Delta P_e}{2\rho V_c^2 \frac{L}{D_h}} \tag{4}$$

3.2. Heat transfer

The average convection heat transfer coefficient is calculated as

$$\bar{h} = \frac{\dot{Q}_{conv}}{A_o(T_w - T_{avg})} \tag{5}$$

where T_w is the average surface temperature and T_{avg} is the average temperature of the air at the test section. The heat transfer performance can be in terms of dimensionless Nusselt number and Colburn j factor as

$$Nu = \frac{\bar{h}D_h}{k} \tag{6}$$

$$j = \frac{h_o}{\rho V_c C_{p_a}} Pr^{2/3} \tag{7}$$

Uncertainties in the reported experimental values were estimated by the method suggested by Moffat [14]. The uncertainties range from 1.15% to 3.69% for the Nu, 1.18–3.71% for the j and 0.82–1.02% for f. The highest uncertainties were associated with lowest Reynolds number.

4. Results and discussion

Test results of pressure drops and heat transfer coefficients vs. frontal velocity for all the test samples are plotted in Fig. 4a and b [15,16]. As expected, both heat transfer coefficients and the pressure drop increases with the rise of frontal velocity. For the increase of pressure drop among the test fin patterns, it can be found that the pressure drops increase considerably when the fin spacing is reduced. However, the effect of fin spacing on the pressure drops is especially pronounced for louver and slit fin geometry. This is associated with the interrupted surface being capable of providing more turbulent mixing of the air flow. Notice that at a very small fin spacing of 0.8 mm, the pressure drop of slit fin is almost identical with that of louver fin geometry. Explanation of this unusual characteristic is due to the tremendous increase of the contribution of a series influence of entrance and exit loss from slit. This can be made clear from a schematic plot of the influence of fin spacing for slit fin in Fig. 5a. As illustrated in Eq. (1), the total pressure drops consisted of entrance, friction and exit loss. For the pure frictional part ΔP_f, the presence of louver re-directs the airflow and eventually leads to a higher contribution of its configuration. However, the relevant contribution of the entrance/exit loss is also increasing when the fin spacing is reduced. Furthermore, one should notice that the contribution of entrance/exit for slit fin geometry increases more dramatically than the louver fin geometry subject to the series combination of the slit configurations. The summation of entrance/exit loss is in fact related to the form drag. Zhang et al. [17] conducted a three-dimensional unsteady simulation of the slit fin geometry having inline and staggered configuration. His calculation clearly indicates that the form drag contrition of the total friction steadily increases with the rise of Reynolds number. This corresponds to the present results.

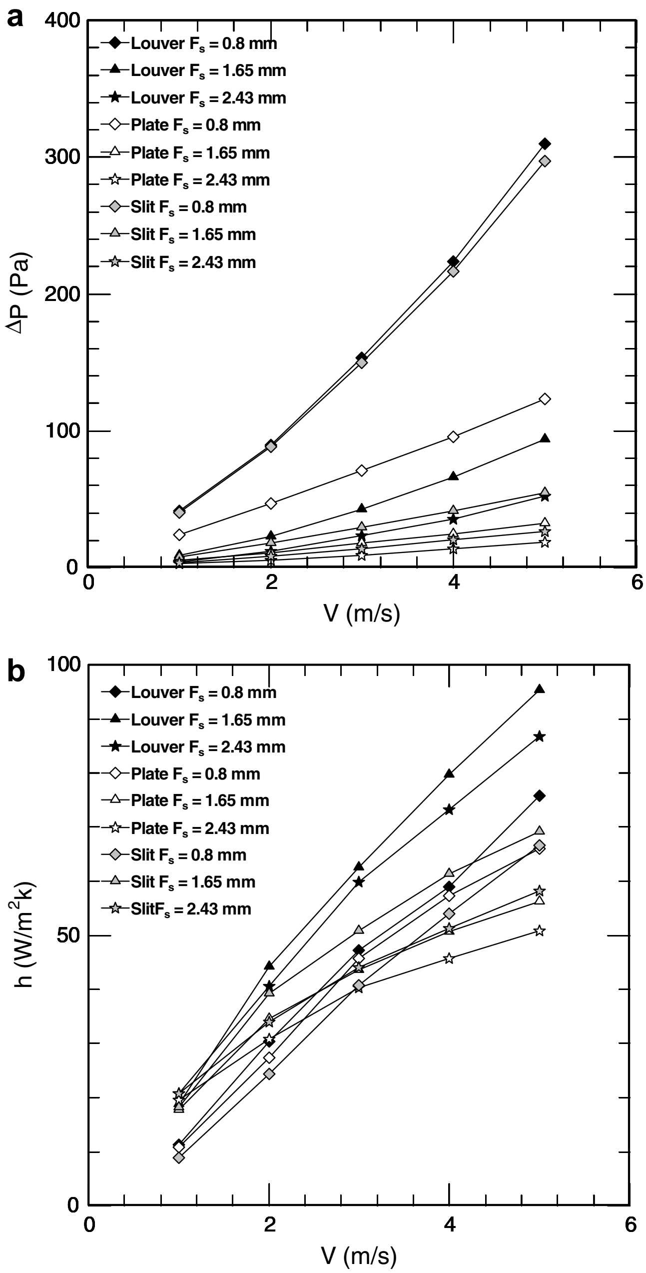

Fig. 4. (a) Pressure drops, (b) heat transfer coefficients vs. frontal velocity for louver, slit and plate fin.

Test results for the heat transfer coefficient for the three fin geometries are shown in Fig. 4b. As seen in the figures, the effect of fin spacing on the heat transfer coefficients is quite different for the tested fin geometries. For plate fin geometry, one can see a detectable increase of heat transfer coefficient when the fin spacing is decreased. Conversely, the heat transfer coefficient for slit fin geometry is increased moderately when the fin spacing is reduced from 2.43 to 1.65 mm, but the corresponding heat transfer coefficients are reduced more than 10% when the fin spacing is further reduced to 0.8 mm. This phenomenon becomes even more severe for louver fin geometry. One can see a slight increase of heat transfer coefficient of 5–10% when the fin spacing is reduced from 2.43 mm to 1.65 mm. However, the heat transfer coefficients undergo a considerable drop at a fin spacing of 0.8 mm. Notice that this phenomenon is even worse at a low frontal velocity. As shown in the figure, an approximate 80% drop of heat transfer coefficient for $F_s = 1.65$ mm relative to $F_s = 0.8$ mm is encountered at $V_{fr} = 1 \text{ m s}^{-1}$. For the louver fin geometry, it is found that the change of heat transfer coefficient is less sensitive to fin spacing provided that the fin pitch is above certain critical value. Some published results had shown a very slight influence of fin pitch [18] in louver fin-and-tube heat exchanger. However, one should notice that the present test louver fin geometry does not have the interactions between fin and tubes.

For further explanation of the significant drop of heat transfer performance at a small fin spacing and at a low Reynolds number, we then examine the associated heat transfer and frictional performance in terms of dimensionless Colburn j factor and Fanning friction factor f vs. Re_{D_h}.

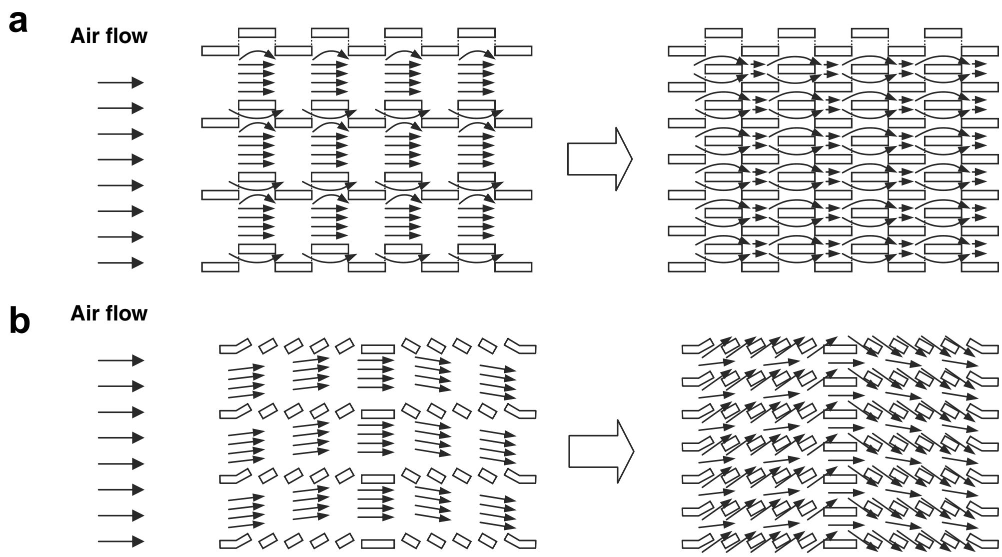

Fig. 5. Schematic of special flow characteristics difference between slit and louver. (a) Effect of periodic entrance/exit loss of slit fin subject to fin spacing of slit fin geometry; (b) duct flow vs. fin-directed flow for louver fin geometry at smaller and larger flow velocities.

As shown in Fig. 6, a very pronounced level-off of the Colburn factor is seen at a fin spacing of 0.8 mm. Actually, a "maximum" Colburn j factor vs. Re_{D_h} had occurred. This is applicable to all the three tested surfaces with the smallest fin spacing of 0.8 mm. The appreciable level-off of the heat transfer coefficient at this low velocity region for the louver fin geometry had been reported by some investigators. For example, Davenport [19] and Achaichia and Cowell [20] had reported that the deterioration of heat transfer coefficients in the low velocities region from their test results of an automotive multi-louver fin surface. Webb and Trauger [21] found that at low Reynolds number some

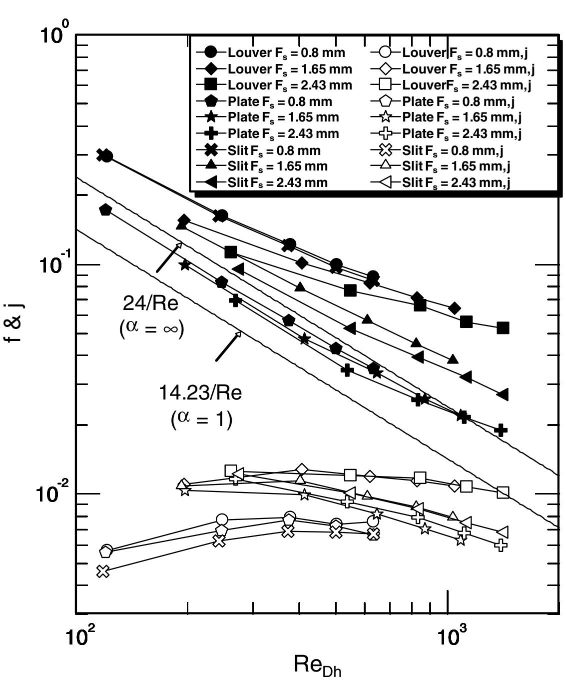

Fig. 6. j & f vs. Re_{D_h} for louver, slit and plate fin.

of the air streams bypass the louvers and act as "duct flow" between the fin channels, giving rise to a lower j factor. Typical flow patterns subject to the influence of velocity can be schematically shown in Fig. 5b. As a result, the improvement of heat transfer performance is rather small in the low frontal velocities region. In addition to this general argument from previous investigators, the present authors found that there is another cause of this heat transfer degradation. Notice that the level-off occurs not only to the louver fin geometry but also to the slit and plate fin geometry as shown in Fig. 6. Notice that Shah and Sekulić [22] had attributed to this phenomenon as the "experimental error". However, the present authors believe that it is a physical phenomenon. For further illustration of this phenomenon, one can examine the corresponding reciprocal of the inverse Graetz number x^+, which is defined as

$$x^+ = \frac{L/D_h}{Re_{D_h} Pr} \tag{8}$$

where L is the streamwise duct length and Pr is the Prandtl number. The flow may be considered to be fully developed when $x^+ > 0.1$ [23]. For further comparison about the influence of developing flow on the heat transfer performance, test results are plotted in terms j vs. the inverse Graetz number as shown in Fig. 7. The right hand side of the ordinate ($x^+ > 0.1$) denotes the flow region being fully developed whereas the region $x^+ < 0.1$ represents the developing region. By carefully examining the test results, we find out that the test results at the lower Reynolds number fall within the fully developed region where a considerable drop of heat transfer performance can be easily explained. In the meantime, the heat transfer performance in the developing region reveals a much better heat transfer performance. In summary of these two distinct heat transfer characteristics, resulting in a maximum phenomenon of j

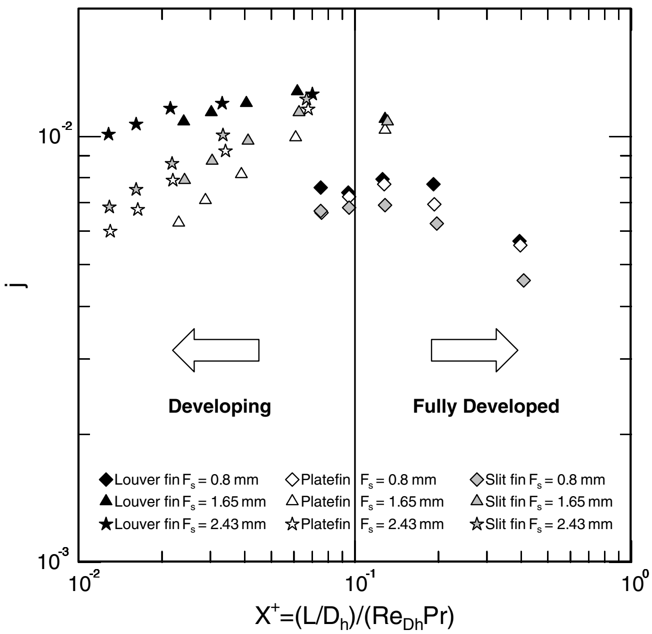

Fig. 7. Inverse Graetz number x^+ vs. j for louver, slit, and plate fin.

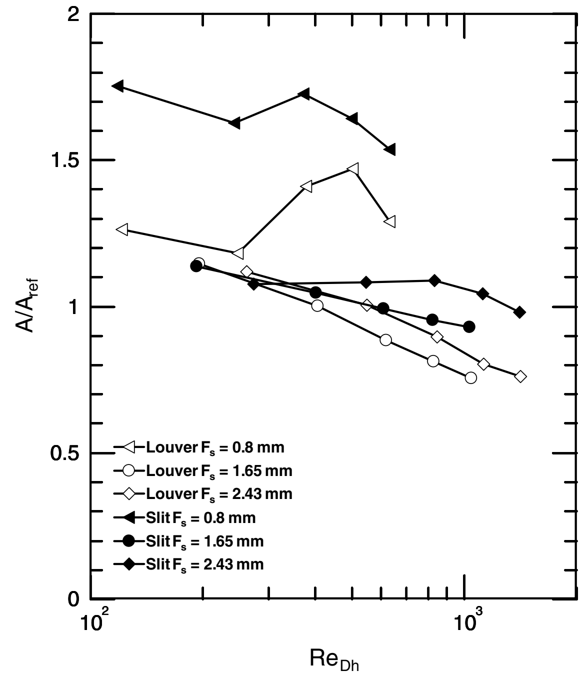

Fig. 8. Required heat-dissipation surface area ratios between louver, slit and plate fin subject to VG-1 criteria.

vs. Re_{D_h}. The maximum position corresponds roughly to the point separating the region of fully developed and developing. This is applicable to all the fin geometries tested. This is because that in low velocity region the highly interrupted surface like louver acts like a duct flow [21], therefore no considerable differences are shown. The results imply a difficult situation of heat transfer augmentation occurring at the low velocity having smaller fin spacing. As explained earlier, the poor heat transfer performance is expected for its fully developed nature. However, augmentation like louver or slit fin also can not do any good subject to the "duct flow" nature in the low velocity region. Therefore, one can see that augmentation in this region only gives rise to significant pressure drop penalty without the benefits of appreciable heat transfer enhancement.

Also shown in Fig. 6 is the associated frictional performance. For comparison purpose, the fully developed friction factor for a square channel and a parallel plate is also plotted in the figure. These lines are based on the simplified polynomial proposed by Hartnett and Kostic [24] that is capable of describing the friction factor inside rectangular cross section for laminar flow

$$f = \frac{24(1 - 1.3553\alpha + 1.9467\alpha^2 - 1.7012\alpha^3 + 0.9564\alpha^4 - 0.2537\alpha^5)}{Re_{D_h}} \tag{9}$$

where α is the aspect ratio of the rectangular section, and the Reynolds number, Re_{D_h}, is based on hydraulic diameter, and is termed as

$$Re_{D_h} = \frac{\rho V D_h}{\mu} \tag{10}$$

For plate fin geometry, the measured friction factor is within these two limits (parallel plate and square channel) except for the results of $F_s = 2.43$ mm at $Re_{D_h} > 1000$. One can clearly see that the slope changes its slope when $Re_{D_h} > 600$, suggestion a change of flow pattern thereafter. Relative to the plate fin pattern, the friction factor for enhanced fin patterns are more sensitive to fin spacing. However, the effect diminishes with the rise of Reynolds number. This is again attributed to the foregoing explanations of the degradation of heat transfer performance. Namely the influence of developing/fully developed and duct/fin directed flow.

For further performance evaluation of the tested heat sinks, comparisons are made subject to the VG-1 [25] criteria. As shown in the Fig. 8, the ordinate of the figure is A/A_{ref}. A value above unity indicates that the required surface area for interrupted fin surface design exceeds that of plain fin surface to fulfill the same heat duty at a fixed pumping power. The results shown in this figure suggest that the louver and slit fin operated with a higher frontal velocity and with a larger fin spacing is more beneficial. The effective heat transfer enhancement of louver was better than slit fin. When the Reynolds number is decreased or the pitch of fins is decreased, the required heat dissipation area of louver and slit fin would gradually surpass that of plate fin. The result from the present experiment suggests a fin with fin pitch of 1.65 mm as the optimum enhancement design. The design could reduce 25% required heat dissipation area.

5. Conclusions

This study conducts an experimental study of heat sinks having plate, slit, and louver fin patterns. Comparison of the associated heat transfer performance and the effect of fin spacing are reported in this study. The results indicate that the enhanced fin pattern like louver or slit fin operated at a higher frontal velocity and at a larger fin pitch is more beneficial than that of plain fin geometry. The design of louver is better than that of the slit fin for heat transfer augmentation. Test results show that the best design of louver fin is with a fin spacing of 1.65 mm. The design could reduce 25% required heat dissipation area.

For the interrupted fin geometry like louver or slit, the increase of pressure drop for louver fin is higher than slit fin when the fin spacing is less than 1.65 mm. However, it is found that the pressure drop of the slit fin is comparable to that of louver fin when the fin spacing is reduced to 0.8 mm. This is associated with the appreciable rise of entrance/exit loss (or form drag) caused by the series combination of slit fin geometry.

The test results indicate a significant drop of heat transfer performance at a low Reynolds number and at a small fin spacing. A so-called "maximum" phenomenon of the j factor vs. Reynolds number is encountered. This is applicable to all the tested geometries. By a careful examination of the test results, it is concluded that this phenomenon is related to the developing/fully developed flow pattern. The sudden drop of heat transfer performance is due to the fully developed flow. In fact, the maximum point roughly corresponds to $x^+ = 0.1$ where fully developed and developing flow is separated.

Acknowledgement

The authors would like to express gratitude for the supporting funding from the Department of Industrial Technology, Ministry of Economic Affairs, Taiwan.

References

[1] E.M. Sparrow, B.R. Baliga, S.V. Patankar, Forced convection heat transfer from a shrouded fin array with and without tip clearance, J. Heat Transfer 100 (4) (1978) 572–579.
[2] A. Bar-Cohen, W.M. Rohsenow, Thermally optimum spacing of vertical, natural convection cooled, parallel plates, J. Heat Transfer 106 (1) (1984) 116–123.
[3] A. Bejan, A.M. Morega, Optimal arrays of pin fins and plate fins in laminal forced convection, J. Heat Transfer 115 (1993) 75–81.
[4] P. Teertstra, J.R. Culham, M.M. Yovanovich, Analytical modeling of forced convection in slotted plate fin heat sink, ASME HTD 364 (1) (1999) 3–11.
[5] M. Iyengar, A. Bar-Cohen, Design for manufacturability of SISE parallel-plate forced convection heat sinks, IEEE Trans. Compon. Pack. Technol. 24 (2) (2001) 150–158.
[6] C.J. Shih, G.C. Liu, Optimal design methodology of plate-fin heat sinks for electronic cooling using entropy generation strategy, IEEE Trans. Compon. Pack. Technol. 27 (3) (2004) 551–559.
[7] S. Narasimhan, A. Bar-Cohenm, Fellow, IEEE, R. Nair, Thermal compact modeling of parallel plate heat sinks, IEEE Trans. Compon. Pack. Technol. 26 (1) (2003) 37–146.
[8] B. Boesmans, F. Christiaens, J. Berghmans, E. Beyne, Design of an optimal heat-sink geometry for forced convection air cooling of multichip modules, in: Proc. Eurotherm Seminar No. 29, Thermal Management of Electronic Systems, Delft, The Netherlands, June 14–16, 1993.
[9] Y.J. Chang, K.C. Hsu, Y.T. Lin, C.C. Wang, A generalized friction correlation for louver fin geometry, Int. J. Heat Mass Transfer 43 (12) (2000) 2237–2243.
[10] Y.J. Chang, C.C. Wang, A generalized heat transfer correlation for louver fin geometry, Int. J. Heat Mass Transfer 40 (3) (1997) 533–544.
[11] ASHRAE Handbook Fundamental. SI-Edition, American Society of Heating, Refrigerating and Air-conditioning Engineers, Inc., Atlanta, 1993, pp. 13.14–13.15.
[12] ASHRAE Standard 41.2-1987. Standard Methods for Laboratory Air-flow Measurement, American Society of Heating, Refrigerating and Air-Conditioning Engineers, Inc., Atlanta, 1987.
[13] W.M. Kays, A.L. London, Compact Heat Exchangers, third ed., McGraw-Hill, New York, 1984.
[14] R.J. Moffat, Describing the uncertainties in experimental results, Exp. Therm. Fluid Sci. 1 (1988) 3–17.
[15] N.C. Dejong, A.M. Jacobi, An experimental study of flow and heat transfer in parallel-plate arrays: local, row-by-row and surface average behavior, Int. J. Heat Mass Transfer 40 (6) (1997) 1365–1378.
[16] M. Kajino, M. Hiramatsu, Research and development of automotive heat exchangers, in: W.J. Yang, Y. Mori (Eds.), Heat Transfer in High Technology and Power Engineering, Hemisphere, Washington, DC, 1987, pp. 420–432.
[17] L.W. Zhang, S. Balachandar, D.K. Tafti, F.M. Najjar, Heat transfer enhancement mechanisms in inline and staggered parallel-plate fin heat exchangers, Int. J. Heat Mass Transfer 40 (10) (1997) 2307–2325.
[18] C.C. Wang, C.J. Lee, C.T. Chang, S.P. Lin, Heat transfer and friction correlation for compact louvered fin-and-tube heat exchangers, Int. J. Heat Mass Transfer 42 (11) (1999) 1945–1956.
[19] C.J. Davenport, Correlations for heat transfer and flow friction characteristics of louvered fin, AIChE Symp. Ser. 79 (225) (1983) 19–27.
[20] A. Achaichia, T.A. Cowell, Heat transfer and pressure drop characteristics of flat tube and louvered plate fin surface, Exp. Therm. Fluid Sci. 1 (1988) 147–157.
[21] R.L. Webb, P. Trauger, Flow structure in the louvered fin heat exchanger geometry, Exp. Therm. Fluid Sci. 4 (1991) 205–217.
[22] R.K. Shah, D.P. Sekulić, Heat exchangers, in: W.M. Rohsenow, J.P. Harnett, Y.I. Cho (Eds.), Handbook of Heat Transfer, McGraw-Hill, New York, 1998, p. 17.70 (Chapter 17).
[23] J.E. Sergent, A. Krum, Thermal Management Handbook for Electronic Assemblies, McGraw-Hill, New York, 1998.
[24] J.P. Hartnett, M. Kostic, Heat transfer to Newtonian and non-Newtonian fluids in rectangular ducts, Advances in Heat Transfer, vol. 19, Academic Press, 1989, pp. 247–356.
[25] R.L. Webb, Principles of Enhanced Heat Transfer, John Wiley & Sons Inc., 1994.